Raman microspectrometry of laser-reshaped rabbit auricular cartilage: preliminary study on laser-induced cartilage mineralization

Michal Heger
University of Amsterdam
Academic Medical Center
Laser Center
Amsterdam, The Netherlands
E-mail: M.Heger@amc.uva.nl

Serge Mordon
Lille University Hospital
INSERM EA 2689, IFR 114
Lille, France

Gérard Leroy
Lille University Hospital
Department of Odontology
LBM Raman
Lille, France

Laurence Fleurisse
Colette Creusy
Catholic University
Saint Vincent Hospital
Department of Pathology
Lille, France

Abstract. Laser-assisted cartilage reshaping (LACR) is a relatively novel technique designed to noninvasively and permanently restructure cartilaginous tissue. It is believed that heat-induced stress relaxation, in which a temperature-mediated disruption of H_2O binding is associated with conformational alterations in the proteoglycan and collagen-rich matrix, constitutes the underlying mechanism of LACR. Several reports have suggested that laser-mediated cartilage mineralization may contribute to the permanent shape change of laser-reshaped cartilage. In an effort to validate these results in the context of Er:glass LACR, we performed a preliminary Raman microspectrometric study to characterize the crystal deposits in laser-irradiated chondrocytes and extracellular matrix. For the first time, we identified intracellular calcium sulfate deposits and extracellular calcium phosphate (apatite) crystals in laser-reshaped rabbit auricular cartilage. Calcium carbonate deposits are localized in both irradiated and nonirradiated samples, suggesting that this mineral plays no role in conformational retention. In our discussion, we elaborate on the possible molecular and cellular mechanisms responsible for intra- and extracellular crystallization, and propose a novel hypothesis on the formation of apatite, inasmuch as the biological function of this mineral (providing structure and rigidity in bones and dental enamel) may be extrapolated to the permanent shape change of laser-irradiated cartilage.
[DOI: 10.1117/1.2187420]

Keywords: laser-assisted cartilage reshaping; Raman spectroscopy; mineralization; calcification; apatite; calcium sulfate.

Paper 05232R received Aug. 16, 2005; revised manuscript received Nov. 13, 2005; accepted for publication Nov. 28, 2005; published online Mar. 27, 2006.

1 Introduction

Laser cartilage reshaping (LACR) is a relatively novel technique designed to noninvasively and permanently restructure cartilaginous tissue for applications in otorhinolaryngology, orthopedics, and plastic surgery. Albeit the efficacy of LACR has been empirically demonstrated in animals[1–9] and humans,[10] the specific biophysical and biochemical mechanisms underlying the laser-tissue interactions have remained largely elusive. The current contention is that LACR is mainly governed by laser-induced stress relaxation[2,11,12] in which a temperature-mediated disruption of H_2O binding is associated with conformational alterations in the proteoglycan (PG) and collagen-rich matrix. In a native state, a small percentage of H_2O molecules provides structural integrity by facilitating electrostatic interactions between collagen and PGs.[13] Laser irradiation causes a dissociation of bound H_2O and a corollary reduction in tensile stresses and matrix stability,[14–17] resulting in a shape change of cartilage.

Insofar as the H_2O phase transition cannot be solely responsible for the permanent deformation of cartilage, Sobol et al.[18,19] have postulated that local mineralization may enforce the long-term restructuring process following laser irradiation. In support of this hypothesis, Velegrakis et al.[5] found loci of calcification in CO_2 laser–irradiated auricular cartilage *in vitro*, and Sobol et al.[18] reported on the occurrence of submicrometer sodium carbonate ($NaCO_3$) crystals in the matrix of CO_2 laser–irradiated nasal septal cartilage samples. Since $NaCO_3$ crystals are chemically unstable and resolve in time, the authors dismissed the possibility that local mineralization of this type may contribute to the generation of a stable cartilage configuration.[18] A later *in vivo* study[20] of porcine ear cartilage evinced the presence of crystals of undetermined composition in the irradiated zone 4 months after laser treatment, refuting the notion that laser-induced crystal formation is merely a short-term phenomenon.

In this preliminary study, we aimed to evaluate chronic Er:glass laser–induced mineralization in rabbit auricular cartilage using Raman microspectrometry, an optical technique

Address all correspondence to Serge Mordon, INSERM-EA 2689-IFR 114, Lille University Hospital, Pavillion Vancostenobel, 59037 Lille, France. Tel: +33 320 446907; Fax: +33 320 446907; E-mail: mordon@lille.inserm.fr

1083-3668/2006/11(2)/024003/8/$22.00 © 2006 SPIE

based on inelastic scattering of light by the molecules in a sample. Provided that each molecular species has a specific set of intramolecular bond vibrations,[21] the spectroscopically detected frequency shifts in remitted light function as "optical fingerprints" that can be employed for qualitative analysis of tissue constituents. Raman microspectrometry therefore constitutes a useful technique for studying postinterventional tissular modifications, and in particular for attesting the composition of intra- and extracellular mineral deposits.

2 Materials and Methods

2.1 *Animals*

Two female white New Zealand rabbits weighing 3.1 and 3.5 kg were used in this study. The animals were housed under standard laboratory conditions and maintained on standard laboratory food and water ad libitum. All procedures were approved by the Lille University Animal Ethics Committee (protocol 2003-021) and conducted in compliance with the *Resolution on the Use of Animals in Research* (Ministère de L'Agriculture et de la Forêt, No. 87-848, Agreement No. 4844).

For the experimental procedure, the animals were placed in a restrainer. Rabbit ear lobes were used because of their abundant elastic cartilage content (mean cartilage thickness of 350 μm) and accessibility. The target region of the ear was locally anesthetized by topical application of 2% lidocaine, shaved, and disinfected. The upper third portion of the ear was mechanically deformed by the placement of a preperforated reshaping jig (curvature radius of 5 mm) prior to lasing. A light source was inserted into the reshaping jig so as to standardize laser irradiation by providing target points through transillumination.[8] The animals were sacrificed after the biopsy procedure by intravenous administration of KCl.

2.2 *Laser Treatment*

Laser irradiation was performed with a 1.54 μm Er:glass laser (Aramis, Quantel Medical, Clermont Ferrand, France). The treatment consisted of seven stacked pulses of 12 J/cm^2 per pulse, 3 ms pulse duration, and a 2 Hz repetition rate, yielding an irradiance of 24 W/cm^2 and cumulative radiant exposure of 84 J/cm^2 with a 4 mm spot size. An integrated cooling device (Koolburst, Quantel Medical, Clermont Ferrand, France) was placed in direct contact with the skin. The cooling temperature was set to 5 °C and contact was maintained for approximately 2 s before lasing. Eight contiguous parallel rows along the ear consisting of 12 adjacent, nonoverlapping spots were subjected to irradiation (area of ~3.2 × 5.0 cm). The irradiated region was delineated by tattooing the margins of the treatment zone. For postoperative curvature maintenance, the reshaping jig was replaced by a holder (10 mm diameter plastic tube) and secured with sutures. The holder was removed after 1 week. Curvature radius measurements were performed as reported previously[8] before punch biopsies.

2.3 *Tissue Preparation and Raman Microspectrometry*

Samples were excised by 3 mm punch biopsy at 3 and 6 weeks after laser treatment from the irradiated and nonirradiated (control) sites after application of 2% lidocaine. Six samples were biopsied per site at each time interval and snap frozen by immersion in liquid nitrogen. The excised tissue was cryocut into 10 μm thick sections and stored at −80 °C until further processing. Prior to Raman spectroscopic analysis, the samples were fixed in 4% formaldehyde for 3 min, washed in deionized water, and passively dried.

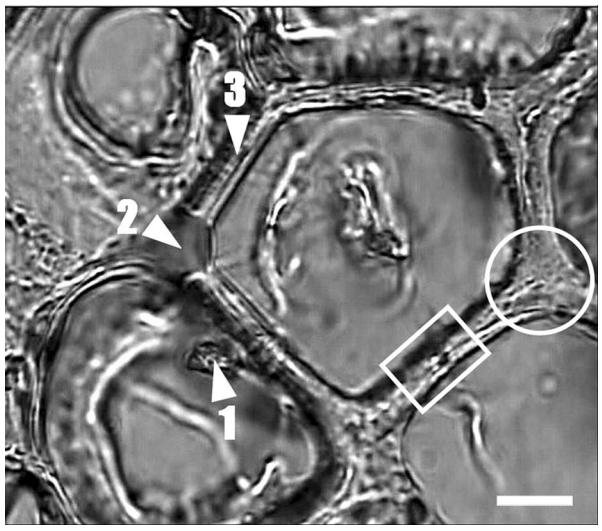

Fig. 1 Histological section of a cartilage sample. Raman spectra were recorded in intracellular crystalline structures (1), at the multicellular Y junctions (2, circle), and at the bicellular I junctions (3, rectangle). Unstained sample, original magnification ×100, scale bar=10 μm.

The samples were analyzed with a Raman microspectrometer (Labram, Jobin Yvon, Lille, France). Spectra were measured in intracellular crystal structures (3 weeks: control, n=6, LACR, n=3; 6 weeks: control, n=5, LACR, n=4) and in the multicellular (Y) and bicellular (I) junctions of the pericellular matrix (Y junction 3 weeks: control, n=9, LACR, n=14; 6 weeks: control, n=9, LACR, n=12; I junction 3 weeks: control, n=7, LACR, n=5; 6 weeks: control, n=4, LACR, n=5) (see Fig. 1). Raman excitation was induced by a HeNe laser (632.8 nm, 8 mW, 1 μm spot size) passed through a narrowband interference filter (FWHM 1 nm, model 03 FIL 006, Melles Griot, Voisins-le-Bretonneux, France) and focused on the region of interest through the microscope optics (BHM brightfield/darkfield metallurgical microscope, Olympus, Rungis, France). Raman signals were collected by the objective lens [100× magnification, numerical aperture (NA) of 0.95] and acquired by a single-grating spectrometer equipped with an air-cooled CCD detector. The overall spectral resolution was 2 Δcm^{-1} in the 250 to 3200 Δcm^{-1} range with an integration time of 100 s. Background fluorescence was subtracted from baseline computations, and polynomial filtering was performed using LabSpec software (Dilor-Jobin Yvon, Lille, France). Raman spectra were normalized to the highest intensity value measured.

3 Results

The outcome of LACR with respect to treatment-related thermal effects and auricular morphology was similar to previous findings:[8] no immediate laser-induced effects such as swelling, erythema, or hypopigmentation were observed macro-

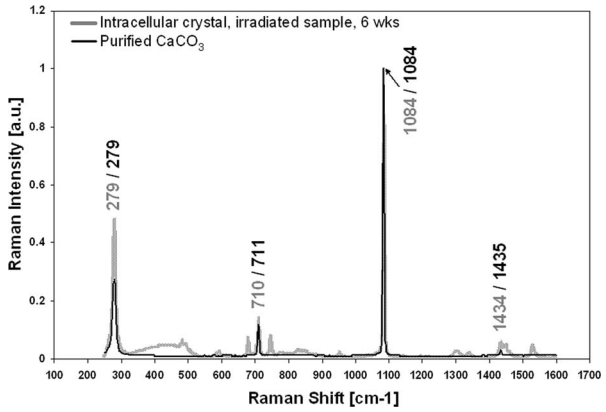

Fig. 2 Raman spectra of an intracellular calcium carbonate (calcite) crystal from a laser-irradiated specimen at $t=6$ weeks (gray). The peaks at 275, 709, and 1083 Δcm^{-1} are characteristic of calcium carbonate, as corroborated by the reference spectrum of purified calcium carbonate (black). Spectra are normalized to the highest intensity value measured.

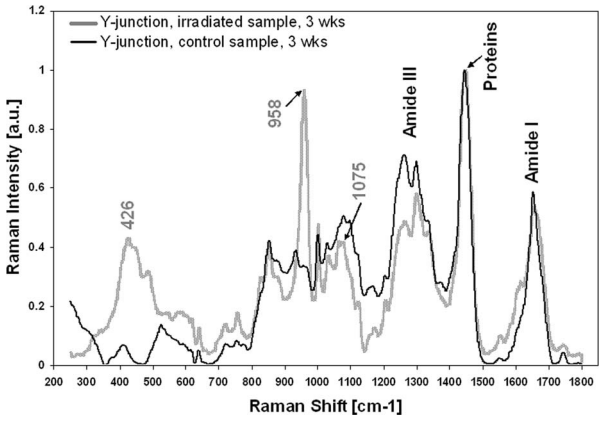

Fig. 4 Raman spectra obtained from a Y junction in a control (black) and a laser-irradiated (gray) specimen at $t=3$ weeks. The prominent apatite peaks at 426 and 958 Δcm^{-1} are present only in the post-LACR sample. The small peak at 1075 Δcm^{-1} indicates a type B carbonate substitution.[25] Proteins (amide I and III, and CH bending modes around 1446 Δcm^{-1}) and other biomolecules (not indicated) were also detected.[22,23] Spectra are normalized to the highest intensity value measured.

scopically, and latent sequelae such as crusting or blistering remained absent. At 3 and 6 weeks the curvature radii were 7.5 and 8.0 mm, respectively, in comparison to the initial curvature radius of the reshaping jig (5 mm).

Histologically, intracellular crystalline structures were found in approximately equal numbers in control and laser-irradiated samples at $t=3$ and 6 weeks. Raman microspectrometry of these intracellular structures revealed that the crystals are predominantly composed of calcium carbonate (calcite, $CaCO_3$) with distinct peaks at 275, 709, and 1083 Δcm^{-1} (Fig. 2). In one of the three irradiated samples at $t=3$ weeks we detected calcium sulfate ($CaSO_4$), characterized by spectral peaks at 412, 491, 617, 668, 1006, 1133 Δcm^{-1} (Fig. 3). $CaSO_4$ was not found in any of the control samples or in the irradiated samples at $t=6$ weeks. In addition, the peaks at 1300 Δcm^{-1} (CH_2 twisting mode, Fig. 3), 1438 Δcm^{-1} (CH_2 bending mode, Fig. 3), 2850 Δcm^{-1} (symmetrical CH_2 stretching, results not shown), and 2893 Δcm^{-1} (asymmetrical CH_2 stretching, results not shown) are indicative of phospholipids.[22,23]

Figure 4 depicts spectra obtained from a Y junction in control (black) and laser-irradiated (gray) specimens at $t=3$ weeks. The peaks at 426 and 958 Δcm^{-1} from the laser-irradiated cartilage sample correspond to the phosphate (PO_4) v_2 and v_1 vibration modes of apatite,[22–27] respectively, which was found in two of the 14 analyzed Y junctions at $t=3$ weeks. A reference spectrum of purified carbonated apatite is provided in Fig. 5. The peak at 1075 Δcm^{-1} (gray spectra, Figs. 4 and 5) suggests a type B substitution (CO_3 substitution of PO_4) in the crystal lattice,[25,26] as is often the

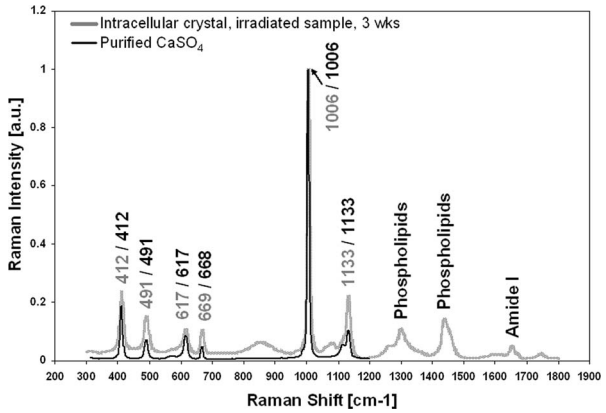

Fig. 3 Raman spectrum of an intracellular calcium sulfate crystal from an irradiated specimen at $t=3$ weeks (gray). Calcium sulfate, with specific peaks at 412, 491, 617, 668, 1006, and 1133 Δcm^{-1}, was found in only one of the seven irradiated samples. For reference, the spectrum of purified calcium sulfate is included (black). Spectra are normalized to the highest intensity value measured.

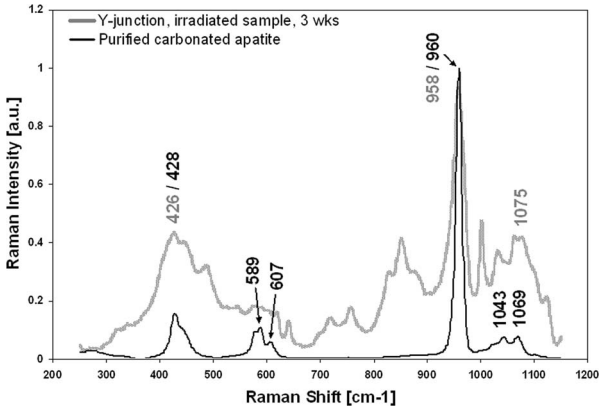

Fig. 5 Laser-irradiated cartilage sample from Fig. 4 (gray) compared to the reference spectrum of purified carbonated apatite (black). The spectra show similar phosphate v_2 and v_1 vibration modes (428 and 960 Δcm^{-1}, respectively), but apatite from the laser-irradiated specimen lacks peaks at 589 and 607 Δcm^{-1} (type A carbonate substitutions), and 1043 Δcm^{-1} (type B carbonate substitution).[25] The peak at 1075 Δcm^{-1} (v_1 vibration mode of carbonate) alludes to a B-type carbonate substitution[25] in the apatite from laser-irradiated specimens. Spectra are normalized to the highest intensity value measured.

case in biological apatites such as bone.[28,29] The bands at 873 and 1001 Δcm^{-1} may be attributed to acidic phosphate ions[22,25] (HPO_4^{2-}). Since OH stretching modes above 3500 Δcm^{-1} (usually present in hydroxyapatite and dental enamel[25,27]) fall outside the detection range, it is impossible to draw irrevocable conclusions on the hydroxylation state of the apatite. No apatite was detected in the control samples, the I junctions at $t=3$ and 6 weeks, and the Y junctions examined at $t=6$ weeks.

4 Discussion

The principal mechanisms underlying the permanent shape change of cartilaginous tissue following laser irradiation have been elaborately investigated[1,2,5,8,9,12,14,18,30–37] since the inception of LACR in 1993. Currently, it is accepted that laser-induced stress relaxation, i.e., the reduction of tensile stresses in the cartilage extracellular matrix (ECM) as a result of a heat-mediated H_2O redistribution and corollary reorganization of intramolecular bonds, lies at the basis of the restructuring machinery. The laser-induced phase transition of H_2O is inevitably accompanied by ancillary processes, including thermally mediated de- and subsequent repolymerization of PG aggregates or its glycosaminoglycan subunits, transient disruption of collagen-PG linkages, and thermal denaturation of matrix proteins such as collagen.[5,18,19,30]

In addition to these acute biochemical events, several recent studies[5,18,20] have revealed that LACR-induced cartilage mineralization may comprise a chronic component of the permanent restructuring process. Inasmuch as the crystal deposits found in these studies were either uncharacterized[5,20] or of a chemically unstable composition,[18] we performed a Raman microspectrometric study to validate the previously obtained results in the context of Er:glass LACR and to identify chemically stable crystal structures in rabbit auricular cartilage 3 and 6 weeks after lasing. Although the results are preliminary due to the limited sample size, we were able to unequivocally identify cytosolic calcium sulfate deposits and extracellular apatite $[Ca_5(PO_4)_3(OH,F,Cl)]$ crystals in the laser-treated samples at $t=3$ weeks by their spectral correspondence to purified analogues (black spectra in Figs. 3 and 5, respectively). On top of the fact that healthy auricular cartilage rarely calcifies, the absence of chondrocalcinosis in the untreated specimens strongly suggests that laser-mediated (auricular) cartilage mineralization is a direct consequence of the photothermal interactions with tissue. In this respect, two main questions must be elucidated: what are the exact dynamics of laser-induced cartilage mineralization? and to what extent does crystal formation contribute to the overall conformational stability of laser-reshaped cartilage? Since our findings have the greatest relevance to the former, the discussion predominantly focuses on laser-induced mineralization processes.

Theoretically, all the acute ultrastructural modifications associated with stress relaxation[5,18,19,30] could invoke a microscale milieu replete with potential nucleation centers required for crystal formation and growth, provided that certain (patho)physicochemical conditions dominate. The most imperative condition for crystal formation is an exceedance of the critical supersaturation level by the component ions. The critical supersaturation represents a value close to the solubility product above which the component ions of the crystal do not remain in solution but precipitate and form aggregates.[38] Cartilage fluids are marginally supersaturated with $CaPO_4$, the main component ion of biological apatite, but do not crystallize due to the presence of chelators and crystallization inhibitors such as proteoglycan aggregates and chondroitin sulfate.[38–41] A laser-induced alteration in the ECM hydration state could therefore shift the supersaturation level toward a higher ionic disequilibrium, producing an environment that significantly favors crystal formation. A representative shift was recently reported by Youn et al.,[42] who, using polarization-sensitive optical coherence tomography, revealed that laser-induced phase retardation changes observed at temperatures of 50 to 78 °C in superficial cartilage layers are primarily attributable to tissue dehydration. Interestingly, these temperatures overlap the temperatures required for stress relaxation (60 to 70 °C).[2,12,14,30,31,34,35] Similarly, a stress-relaxation-associated redistribution of H_2O molecules[1,19,30,31,43] may alter the hydration state locally. The release/relocation of H_2O molecules coincides with the exposure of anionic moieties on the sulfate and carboxyl groups of the glycosaminoglycan chain, which may be electrically neutralized by the binding of Ca^{2+} and Na^+ ions that are abundantly present in cartilage. Since the phase transition of H_2O occurs above the thermal denaturation threshold of collagen (40 to 42 °C) and other matrix proteins, cations may also neutralize negatively charged amino acid residues that are exposed during protein unfolding.[44,45] In addition to the probability that thermal denaturation of crystallization inhibitors will impart an agonistic effect on the mineralization process, the cationic substitution of intermolecular H_2O bonds and intramolecular hydrogen and sulfur bridges is possibly affiliated with the creation of crystal nuclei.[19] Once a crystal is nucleated, lower supersaturation levels are sufficient for crystal growth and proliferation.[38]

The formation of nucleation centers during and immediately after the laser pulse through cationic substitutions is currently the only putative explanation for postirradiative cartilage mineralization.[19] Based on tissue calcification studies in osteology and rheumatology, there is some circumstantial evidence that laser-induced cartilage mineralization in the ECM may be under cellular regulation in addition to the proposed acute biochemical modifications. Nonpathological endochondral ossification, for example, has been mechanistically linked to the release of matrix vesicles (MVs) from apoptotic (hypertrophic) chondrocytes in the epiphyseal growth plate.[46–49] These nanoscale (~100 nm) vesicles are extracellular membrane-enclosed particles that are generated by polarized budding from chondrocytes during early apoptosis.[46,47] The unique intravesicular environment makes MVs optimal mineralization units, particularly with respect to (hydroxy)apatite: the MV cytosolic membrane leaflet is replete with acidic phospholipids (predominantly phosphatidylserine) that promote the ingress of Ca^{2+} ions,[47,50] several types of annexins act as calcium binding proteins and transmembrane calcium channels,[46,47] membrane-embedded phosphohydrolases[47,51–53] control intra- and perivesicular PO_4^{3-} concentrations, and a sodium-dependent PO_4 transporter facilitates ionic uptake.[47,54] A pH regulatory mechanism in the form of carbonic anhydrase provides a basic climate most suitable for

crystal stabilization and sustained growth of preformed hydroxyapatite templates near the inner surface of the MV membrane.[47,55] An equivalent vesicle-mediated mineralization system can be found in degenerative diseases such as osteoarthritis, where chondrocyte-derived apoptotic bodies comprise[56,57] the functional homologues of MVs. The apoptotic bodies, which can be induced *in vitro* by nitric oxide (NO) donors or agonistic antibodies to Fas, a chondrocyte-specific proapoptotic signaling molecule, possess a similar calcification machinery to MVs in that they contain alkaline phosphatase and pyrophosphate-generating nucleoside triphosphate pyrophosphohydrolase activity and have the ability to precipitate calcium ions.[56,57]

With cell death at the basis of physiological and pathological cartilage mineralization, it is not unlikely that laser-induced chondrocalcinosis in the ECM is mediated via common molecular pathways and crystallization processes. Several flow cytometric and histological studies[5,9,58–61] have demonstrated that chondrocyte viability is partially compromised following subablative laser irradiation, with a decrease in cell viability occurring near a temperature threshold of 54 to 56 °C.[59,62] Although the mechanisms of laser-induced chondrocyte death are yet to be irrefutably established, membrane permeability–based live/dead assays of isolated laser-irradiated chondrocytes suggest a necrotic (cell membrane thermolysis and possibly thermal denaturation of cytoplasmic elements) *and* apoptotic origin.[59,61,62] Wong et al.[61] recently identified a subpopulation of cultured chondrocytes 2 and 3 weeks after Nd:YAG laser irradiation that, based on flow cytometric light scattering properties, displayed an apoptotic phenotype. The extent of apoptosis seemed to be positively correlated to irradiation times, i.e., the volumetric heat production. Inasmuch as heat-induced disintegration of the cell membrane causes efflux of cellular contents into the ECM, the release of physiologically active compounds such as NO by dead or injured cells may induce a host of deleterious cellular responses, including oxidative stress, oxidant injury, and apoptosis in neighboring, intact chondrocytes.[56,63–65] Hyperthermic damage to cytosolic polypeptides and proteins may lead to activation of apoptotic signal transduction pathways even in the absence of membrane disruption (the differential thermodestructive criteria between proteins, lipoproteins, and membranes emanate from the thermodynamically stabilizing properties of phospholipids[66]). During severe heat stress ($>$43 to 45 °C), apoptogenic nuclear transcription factors are upregulated by two subfamilies of mitogen-activated protein kinases (MAPKs), namely, p38MAPK and SAPK/JNK, in response to the stress-induced dissociation of apoptosis signal-regulating kinase-1 (Ask1) from its inhibitor GSTM1-1 (glutathione S-transferase Mul-1).[67–70] At the level of the unfolded protein response (UPR), a ubiquitously conserved countermechanism against unfolded or misfolded protein accumulation in the endoplasmic reticulum, three known apoptotic cascades governed by IRE1, caspase-12, and PERK/CHOP are initiated when the protein overload cannot be resolved.[71] Excessive thermal denaturation of nascent polypeptides and preproteins could therefore trigger apoptosis if the UPR, in cooperation with stress-inducible heat shock proteins (HSPs), is ultimately ineffective. Other molecular triggers leading to programmed cell death, including HSP-facilitated degradation of death regulatory proteins,[72] may also play a role in the pathophysiological fate of laser-irradiated chondrocytes. On initiation of the apoptotic program, cells undergo nuclear and cytoplasmic condensation, blebbing, and the formation of apoptotic bodies. The exocytosolic membrane surface of apoptotic bodies becomes replete with target receptors for phagocytosis.[73] Cartilage is unique in the sense of being avascular and lacking phagocytes responsible for engulfing cellular debris and apoptotic bodies,[56] which implies that apoptotic bodies enjoy a relatively long life span in this tissue with ample time to develop mineral templates. Ultimately, in the absence of phagocytosis, apoptotic bodies may proceed to secondary or apoptotic necrosis characterized by a loss of membrane integrity,[73] but probably not before having fulfilled their function as mineralization units.

Taken all together, our Raman microspectrometric characterization of extracellular apatite in the Y junctions of laser-irradiated cartilage specimens fits the mineralization paradigm just outlined. Apatite is a geographically foreign material in the context of auricular cartilage; only 13 clinical cases on auricular cartilage calcification have been reported since 1890, none of which had an alleged etiology associated with severe hyperthermia.[74] The absence of biomineralization in the ECM (Y and I junctions) of control samples therefore indicates that mineralization occurred in response to laser irradiation. Additional support for our hypothesis is derived from the possible connection between laser-induced chondrocyte damage and chondrocalcinosis, with necrosis and apoptosis as the common denominators. Moreover, cartilage tissue constitutes an optimal niche for apoptotic bodies, which can thrive in the ECM without being attacked by inflammatory scavengers of the reticuloendothelial system. The formation of biological apatite in laser-reshaped cartilage may be pertinent to LACR insofar as the sole physiological purpose of $CaPO_4$ crystallization is to impose structure and rigidity during the development of the skeletal framework and dental enamel. These properties could potentially be extrapolated to the chronic shape retention of laser-irradiated cartilage, where local tissue petrification could deter a conformational relapse to the original shape over time.

Contrary to apatite, the biochemical origin and clinical relevance of intracellular calcium sulfate deposits are elusive, particularly because $CaSO_4$ has no apparent intrinsic physiological or structural value. The negative results from extensive Boolean searches using the major search engines (PubMed, ISI Web of Science, and Google) hence suggest that $CaSO_4$ crystal formation in laser-treated chondrocytes is an end result of severely disrupted cellular homeostasis. A condition of cytoplasmic hypercalcemia, concurrently accounting for a local exceedance of the critical supersaturation level, can be justified by the abundant cytosolic and intraorganellar presence of calcium ions and their liberation from intracellular stores following a laser-induced stimulus. However, it is unclear as to how a similar condition in regard to sulfate is established. Individual cells acquire this highly dissociated, divalent hydrophilic anion predominantly from serum via cell-specific transmembrane transport systems and, to a lesser extent, by hydrolysis of sulfoconjugates and oxidation of reduced organic sulfur.[75] The available inorganic sulfate is subsequently metabolized into intracellular sulfate-containing nucleotides, e.g., adenosine 3′-phosphate 5′-sulfatophosphate (PAPS), that act as sulfate donors in various types of sulfation

reactions required for the synthesis of numerous biologically active compounds and for posttranslational modifications of structural components of membranes and tissues[75] (i.e., sulfated glycosaminoglycans, the main constituents of cartilage). Its availability as a component ion for the mineralization process is therefore restricted, unless photothermal damage induces an increased rate of hydrolysis of conjugated sulfate groups, oxidation of organic sulfur, or accelerated influx of sulfate ions from the extracellular environment. It is known that membrane fluidity, i.e., membrane motional order or lipid packing order, affects the passive permeability properties of membranes and the activity and kinetics of membrane-embedded transport carriers.[76,77] Since one of the affectors of membrane fluidity is temperature, the generation of isotherms as a result of light absorption by water might have altered the transmembrane transport kinetics of sulfate ions. Note that these speculations are based on very few related studies. Unfortunately, sulfate is the least-studied serum ion, and little is known about the factors that govern sulfate homeostasis in animals.[78]

5 Conclusion

In this preliminary study, Raman microspectrometry was employed to qualify biominerals in laser-reshaped rabbit auricular cartilage 3 and 6 weeks after Er:glass laser irradiation in an attempt to elucidate the potential role of chondrocalcinosis in LACR. In addition to the previously reported occurrence of sodium carbonate crystals in laser-irradiated porcine nasal septal cartilage,[18] our report presents evidence that laser-induced cartilage mineralization also includes intracellular calcium sulfate and extracellular calcium phosphate crystallization. We were also able to localize calcium carbonate deposits in both control and laser-irradiated samples, which, due to their equiquantitative distribution and intracellular occurrence, probably do not contribute to the permanent shape change of laser-reshaped cartilage. The limited knowledge on laser-induced cartilage mineralization prompted us to explore potential biochemical and molecular origins of chondrocalcinosis outside the thermal stress relaxation framework, also with the intent to pave the way for additional research in this field. We proposed a novel hypothesis on the formation of apatite that is based on photothermally induced necrosis and apoptosis and apoptotic body-mediated mineralization. Conversely, the exact mechanism of intracellular calcium sulfate crystallization remains elusive, and warrants further validation and investigation. Most importantly, the efficacy of LACR as a function of laser-induced biomineralization must be clarified, particularly in ratio to the discussed acute biochemical effects associated with stress relaxation. Once a positive correlation has been established, testing of the hypotheses formulated in this paper should be initiated to devise LACR-enhancing therapeutic modalities.

Acknowledgments

M. Heger was in part supported by the Technological Collaboration Grant No. TSGE 1048 of the Dutch Ministry of Economic Affairs. The authors wish to thank Drs. S. Vilette (Laser Center, Academic Medical Center, University of Amsterdam, Amsterdam, The Netherlands) and G. Penel (LBM Raman, Department of Odontology, Lille University Hospital, Lille, France) for careful review of the manuscript and Prof. A. Boskey (Hospital for Special Surgery, New York) for constructive input on cartilage mineralization.

References

1. E. Helidonis, E. Sobol, G. Kavvalos, J. Bizakis, P. Christodoulou, G. Velegrakis, J. Segas, and V. Bagratashvili, "Laser shaping of composite cartilage grafts," *Am. J. Otolaryngol.* **14**, 410–412 (1993).
2. E. N. Sobol, V. V. Bagratashvili, A. Omelchenko, A. P. Sviridov, E. S. Helidonis, G. Kavvalos, P. N. Christodoulou, I. Naoumidi, G. Velegrakis, Y. M. Ovchinnikov, and A. Shechter, "Laser shaping of cartilage," *Proc. SPIE* **2128**, 43–49 (1994).
3. Z. Wang, M. M. Pankratov, D. F. Perrault, and S. M. Shapshay, "Laser-assisted cartilage reshaping: in vitro and in vivo animal studies," *Proc. SPIE* **2395**, 296–302 (1995).
4. B. J. Wong, T. E. Milner, A. Harrington, J. Ro, X. Dao, E. N. Sobol, and J. S. Nelson, "Feedback-controlled laser-mediated cartilage reshaping," *Arch. Facial Plast. Surg.* **1**, 282–287 (1999).
5. G. A. Velegrakis, C. E. Papadakis, A. A. Nikolidakis, E. P. Prokopakis, M. E. Volitakis, I. Naoumidi, and E. S. Helidonis, "In vitro ear cartilage shaping with carbon dioxide laser: an experimental study," *Ann. Otol. Rhinol. Laryngol.* **109**, 1162–1166 (2000).
6. N. Jones, A. Sviridov, E. Sobol, A. Omelchenko, and J. Lowe, "A prospective randomised study of laser reshaping of cartilage in vivo," *Lasers Med. Sci.* **16**, 284–290 (2001).
7. J. C. Chang, S. Diaz-Valdes, and B. J. F. Wong, "Preliminary investigations of laser-mediated cartilage reshaping in the in-vivo rabbit model," *Proc. SPIE* **4609**, 326–330 (2001).
8. S. Mordon, T. Wang, L. Fleurisse, and C. Creusy, "Laser cartilage reshaping in an in vivo rabbit model using a 1.54 microm Er:Glass laser," *Lasers Surg. Med.* **34**, 315–322 (2004).
9. A. M. Karamzadeh, J. C. Chang, S. Diaz, T. E. Milner, and B. J. Wong, "Long-term in vivo stability of rabbit nasal septal cartilage following laser cartilage reshaping: a pilot investigation," *Lasers Surg. Med.* **36**, 147–154 (2005).
10. Y. Ovchinnikov, E. Sobol, V. Svistushkin, A. Shekhter, V. Bagratashvili, and A. Sviridov, "Laser septochondrocorrection," *Arch. Facial Plast. Surg.* **4**, 180–185 (2002).
11. E. Helidonis, E. N. Sobol, G. Velegrakis, and J. Bizakis, "Shaping of nasal septal cartilage with the carbon dioxide laser—preliminary report of an experimental study," *Lasers Med. Sci.* **9**, 51–54 (1994).
12. E. N. Sobol, V. N. Bagratashvili, A. P. Sviridov, A. I. Omelchenko, A. B. Shekhter, M. I. Isaev, and V. G. Zenger, "Study of cartilage reshaping with a holmium laser," *J. Opt. Soc. Am.* **2623**, 544–547 (1996).
13. A. Maroudas and R. Schneiderman, "'Free' and 'exchangeable' or 'trapped' and 'non-exchangeable' water in cartilage," *J. Orthop. Res.* **5**, 133–138 (1987).
14. B. Wong, T. Milner, B. Anvari, A. Sviridov, A. Omel'chenko, V. Bagratashvili, E. Sobol, and J. S. Nelson, "Thermooptical response of cartilage during feedback-controlled laser-assisted reshaping," *Proc. SPIE* **2970**, 380–391 (1997).
15. E. N. Sobol, M. S. Kitai, N. Jones, A. P. Sviridov, T. Milner, and B. Wong, "Theoretical modelling of heating and structure alterations in cartilage under laser radiation with regard of water evaporation and diffusion dominance," *Proc. SPIE* **3254**, 54–63 (1998).
16. A. M. Jamieson, J. Blackwell, H. Reihanian, H. Ohno, R. Gupta, D. A. Carrino, A. I. Caplan, L. H. Tang, and L. C. Rosenberg, "Thermal and solvent stability of proteoglycan aggregates by quasielastic laser light-scattering," *Carbohydr. Res.* **160**, 329–341 (1987).
17. J. E. Scott, "Proteoglycan-fibrillar collagen interactions," *Biochem. J.* **252**, 313–323 (1988).
18. E. Sobol, A. Omel'chenko, M. Mertig, and W. Pompe, "Scanning force microscopy of the fine structure of cartilage irradiated with a CO_2 laser," *Lasers Med. Sci.* **15**, 15–23 (2000).
19. E. Sobol, A. Sviridov, A. Omel'chenko, V. Bagratashvili, M. Kitai, S. E. Harding, N. Jones, K. Jumel, M. Mertig, W. Pompe, Y. Ovchinnikov, A. Shekhter, and V. Svistushkin, "Laser reshaping of cartilage," *Biotechnol. Genet. Eng. Rev.* **17**, 553–578 (2000).
20. E. N. Sobol, A. P. Sviridov, V. N. Bagratashvili, A. I. Omel'chenko, Y. M. Ovchinnikov, A. B. Shekhter, V. M. Svistushkin, and A. N. Shinaev, "Laser reshaping of nasal septum cartilage: clinical results for 40 patients," *Proc. SPIE* **3907**, 297–302 (2000).
21. E. B. Hanlon, R. Manoharan, T. W. Koo, K. E. Shafer, J. T. Motz, M.

Fitzmaurice, J. R. Kramer, I. Itzkan, R. R. Dasari, and M. S. Feld, "Prospects for in vivo Raman spectroscopy," *Phys. Med. Biol.* **45**, R1–R59 (2000).
22. R. J. Lakshmi, M. Alexander, J. Kurien, K. K. Mahato, and V. B. Kartha, "Osteoradionecrosis (ORN) of the mandible: a laser Raman spectroscopic study," *Appl. Spectrosc.* **57**, 1100–1116 (2003).
23. H. P. Buschman, G. Deinum, J. T. Motz, M. Fitzmaurice, J. R. Kramer, A. van der Laarse, A. V. Bruschke, and M. S. Feld, "Raman microspectroscopy of human coronary atherosclerosis: biochemical assessment of cellular and extracellular morphologic structures in situ," *Cardiovasc. Pathol.* **10**, 69–82 (2001).
24. G. Penel, G. Leroy, C. Rey, B. Sombret, J. P. Huvenne, and E. Bres, "Infrared and Raman microspectrometry study of fluor-fluor-hydroxy and hydroxyl-apatite powders," *J. Mater. Sci.: Mater. Med.* **8**, 271–276 (1997).
25. G. Penel, G. Leroy, C. Rey, and E. Bres, "MicroRaman spectral study of the PO_4 and CO_3 vibrational modes in synthetic and biological apatites," *Calcif. Tissue Int.* **63**, 475–481 (1998).
26. G. Penel, C. Delfosse, M. Descamps, and G. Leroy, "Composition of bone and apatitic biomaterials as revealed by intravital Raman microspectroscopy," *Bone (N.Y.)* **36**, 893–901 (2005).
27. J. D. Pasteris, B. Wopenka, J. J. Freeman, K. Rogers, E. Valsami-Jones, J. A. M. van der Houwen, and M. J. Silva, "Lack of OH in nanocrystalline apatite as a function of degree of atomic order: implications for bone and biomaterials," *Biomaterials* **25**, 229–238 (2004).
28. R. Z. Legeros, "Biological and synthetic apatites," in *Hydroxyapatites and Related Compounds*, P. Brown and B. Constantz, Eds., pp. 3–28, CRC Press, Boca Raton, FL (1994).
29. C. Rey, B. Collins, T. Goehl, R. I. Dickson, and M. J. Glimcher, "The carbonate environment in bone mineral. A resolution enhanced Fourier transform infrared spectroscopy study," *Calcif. Tissue Int.* **45**, 414–420 (1989).
30. E. Sobol, A. Sviridov, V. Bagratashvili, A. Omel'chenko, M. Kitai, and V. Popov, "Mechanism of laser-induced stress-relaxation in cartilage," *Proc. SPIE* **2975**, 310–315 (1997).
31. V. N. Bagratashvili, E. N. Sobol, A. P. Sviridov, A. I. Omel'chenko, and V. K. Popov, "Thermal and diffusion processes in laser-induced stress relaxation and reshaping of cartilage," *J. Biomech.* **30**, 813–817 (1997).
32. A. Sviridov, E. Sobol, N. Bagratashvili, A. Omel'chenko, N. Jones, and J. Lowe, "Dynamics of optical and mechanical properties of cartilage at laser heating," *Proc. SPIE* **2923**, 114–117 (1996).
33. B. Wong, T. Milner, B. Anvari, A. Sviridov, A. Omelchenko, V. Bagratashvili, E. Sobol, and J. S. Nelson, "Measurement of radiometric surface temperature and integrated backscattered light intensity during feedback-controlled laser-assisted cartilage reshaping," *Lasers Med. Sci.* **13**, 66–72 (1998).
34. B. Wong, T. Milner, H. Kim, S. A. Telenkov, C. F. Chew, E. Sobol, and J. Nelson, "Characterization of temperature-dependent biophysical properties during laser-mediated cartilage reshaping," *IEEE J. Sel. Top. Quantum Electron.* **5**, 1095–1102 (1999).
35. A. P. Sviridov, E. N. Sobol, N. Jones, and J. Lowe, "Effect of holmium laser irradiation on stress, temperature, and structure in cartilage," *Lasers Med. Sci.* **13**, 73–78 (1998).
36. B. Wong, T. Milner, H. Kim, J. Nelson, and E. Sobol, "Stress relaxation of porcine septal cartilage during Nd:YAG laser irradiation: mechanical, optical, and thermal responses," *J. Biomed. Opt.* **3**, 409–414 (1998).
37. E. Sobol, M. Kitai, N. Jones, A. Sviridov, T. Milner, and B. Wong, "Heating and structure alterations in cartilage under laser irradiation with regard of water evaporation," *Quantum Electron.* **35**, 532–538 (1999).
38. A. L. Boskey, "Pathogenesis of cartilage calcification: mechanisms of crystal deposition in cartilage," *Curr. Rheumatol. Rep.* **4**, 245–251 (2002).
39. J. Gokhale, P. G. Robey, and A. L. Boskey, "The biochemistry of bone," in *Osteoporosis*, R. Marcus, D. Feldman, and J. Kelsey, Eds., pp. 107–109, Academic Press, New York (2001).
40. G. K. Hunter, M. D. Grynpas, P. T. Cheng, and K. P. Pritzker, "Effect of glycosaminoglycans on calcium pyrophosphate crystal formation in collagen gels," *Calcif. Tissue Int.* **41**, 164–170 (1987).
41. C. C. Chen, A. L. Boskey, and L. C. Rosenberg, "The inhibitory effect of cartilage proteoglycans on hydroxyapatite growth," *Calcif. Tissue Int.* **36**, 285–290 (1983).
42. J. I. Youn, G. Vargas, B. J. F. Wong, and T. E. Milner, "Depth-resolved phase retardation measurements for laser-assisted nonablative cartilage reshaping," *Phys. Med. Biol.* **50**, 1937–1950 (2005).
43. V. Bagratashvili, N. Bagratashvili, A. Sviridov, E. Sobol, A. Omel'chenko, S. Tsypina, V. Gapontsev, I. Smartsev, F. Feldchtein, and R. Kuranov, "Kinetics of water transfer and stress relaxation in cartilage heated with 1.56 μm fiber laser," *Proc. SPIE* **3914**, 102–107 (2000).
44. R. Dong, X. Yan, X. Pang, and S. Liu, "Temperature-dependent Raman spectra of collagen and DNA," *Spectrochim. Acta, Part A* **60**, 557–561 (2004).
45. T. V. Belopolskaya, G. I. Tsereteli, N. A. Grunina, and O. L. Vavelíouk, "DSC study of the postdenatured structures in biopolymer-water systems," *J. Therm Anal. Calorim.* **62**, 75–88 (2000).
46. H. C. Anderson, "Molecular biology of matrix vesicles," *Clin. Orthop. Relat. Res.* **314**, 266–280 (1995).
47. H. C. Anderson, "Matrix vesicles and calcification," *Curr. Rheumatol. Rep.* **5**, 222–226 (2003).
48. H. C. Anderson, R. Garimella, and S. E. Tague, "The role of matrix vesicles in growth plate development and biomineralization," *Front. Biosci.* **10**, 822–837 (2005).
49. K. Johnson, K. Pritzker, J. Goding, and R. Terkeltaub, "The nucleoside triphosphate pyrophosphohydrolase isozyme PC-1 directly promotes cartilage calcification through chondrocyte apoptosis and increased calcium precipitation by mineralizing vesicles," *J. Rheumatol.* **28**, 2681–2691 (2001).
50. N. S. Peress, H. C. Anderson, and S. W. Sajdera, "The lipids of matrix vesicles from bovine fetal epiphyseal cartilage," *Calcif. Tissue Res.* **14**, 275–281 (1974).
51. S. Y. Ali, S. W. Sajdera, and H. C. Anderson, "Isolation and characterization of calcifying matrix vesicles from epiphyseal cartilage," *Proc. Natl. Acad. Sci. U.S.A.* **67**, 1513–1520 (1970).
52. S. Kanabe, H. H. T. Hsu, R. N. A. Cecil, and H. C. Anderson, "Electron microscopic localization of adenosine triphosphate (ATP) hydrolyzing activity in isolated matrix vesicles and reconstituted vesicles from calf cartilage," *J. Histochem. Cytochem.* **31**, 462–470 (1983).
53. H. H. T. Hsu, "Purification and partial characterization of ATP-pyrophosphohydrolase from fetal bovine epiphyseal cartilage," *J. Biol. Chem.* **258**, 3463–3464 (1983).
54. C. Montessuit, J. Caverzasio, and J. P. Bonjour, "Characterization of a Pi transport system in cartilage matrix vesicles: potential role in the calcification process," *J. Biol. Chem.* **266**, 17791–17797 (1991).
55. D. J. Stechschulte, D. C. Morris, S. F. Silverton, H. C. Anderson, and H. K. Vaananen, "Presence and specific concentration of carbonic anhydrase II in rat matrix vesicles," *Bone Miner.* **17**, 187–191 (1992).
56. S. Hashimoto, R. L. Ochs, F. Rosen, J. Quach, G. McCabe, J. Solan, J. E. Seegmiller, R. Terkeltaub, and M. Lotz, "Chondrocyte-derived apoptotic bodies and calcification of articular cartilage," *Proc. Natl. Acad. Sci. U.S.A.* **95**, 3094–3099 (1998).
57. M. Lotz, S. Hashimoto, and K. Kühn, "Mechanisms of chondrocyte apoptosis," *Osteoarthritis Cartilage* **7**, 389–391 (1999).
58. M. Frenz, B. J. Züger, D. Monin, C. Weiler, P. Mainil-Varlet, H. P. Weber, and T. Schaffner, "Laser-induced cartilage damage: an ex-vivo model using confocal microscopy," *Proc. SPIE* **3601**, 115–120 (1999).
59. S. H. Diaz, J. S. Nelson, and B. J. F. Wong, "Rate process analysis of thermal damage in cartilage," *Phys. Med. Biol.* **48**, 19–29 (2003).
60. A. Rasouli, C. H. Sun, R. Basu, and B. J. F. Wong, "Quantitative assessment of chondrocyte viability after laser-mediated reshaping: a novel application of flow cytometry," *Lasers Surg. Med.* **32**, 3–9 (2003).
61. B. J. Wong, N. Pandhoh, M. T. Truong, S. Diaz, K. Chao, S. Hou, and D. Gardiner, "Identification of chondrocyte proliferation following laser irradiation, thermal injury, and mechanical trauma," *Lasers Surg. Med.* **37**, 89–96 (2005).
62. B. J. Züger, B. Ott, P. Mainil-Varlet, T. Schaffner, J. F. Clémence, H. P. Weber, and M. Frenz, "Laser solder welding of articular cartilage: tensile strength and chondrocyte viability," *Lasers Surg. Med.* **28**, 427–434 (2001).
63. F. J. Blanco, R. L. Ochs, H. Schwarz, and M. Lotz, "Chondrocyte apoptosis induced by nitric oxide," *Am. J. Pathol.* **146**, 75–85 (1995).
64. M. Lotz, "The role of nitric oxide in articular cartilage damage," *Rheum. Dis. Clin. North Am.* **25**, 269–282 (1999).
65. R. M. Clancy, S. B. Abramson, C. Kohne, and J. Rediske, "Nitric oxide attenuates cellular hexose monophosphate shunt response to

oxidants in articular chondrocytes and acts to promote oxidant injury," *J. Cell Physiol.* **172**, 183–191 (1997).
66. A. R. Tall, D. M. Small, G. Shipley, and R. S. Lees, "Apoprotein stability and lipid-lipid protein interactions in human plasma high density lipoproteins," *Proc. Natl. Acad. Sci. U.S.A.* **72**, 4940–4942 (1975).
67. S. Dorion, H. Lambert, and J. Landry, "Activation of the p38 signaling pathway by heat shock involves the dissociation of glutathione S-transferase Mu from Ask1," *J. Biol. Chem.* **277**, 30792–30797 (2002).
68. Z. Xia, M. Dickens, J. Raingeaud, R. J. Davis, and M. E. Greenberg, "Opposing effects of ERK and JNK-p38 MAP kinases on apoptosis," *Science* **270**, 1326–1331 (1995).
69. T. Wada and J. M. Penninger, "Mitogen-activated protein kinases in apoptosis regulation," *Oncogene* **23**, 2838–2849 (2004).
70. S. V. Kyosseva, "Mitogen-activated protein kinase signaling," *Int. Rev. Neurobiol.* **59**, 201–220 (2004).
71. K. Zhang and R. J. Kaufman, "Signaling the unfolded protein response from the endoplasmic reticulum," *J. Biol. Chem.* **279**, 25935–25938 (2004).
72. A. Parcellier, S. Gurbuxani, E. Schmitt, E. Solary, and C. Garrido, "Heat shock proteins, cellular chaperones that modulate mitochondrial cell death pathways," *Biochem. Biophys. Res. Commun.* **304**, 505–512 (2003).
73. S. L. Fink and B. T. Cookson, "Apoptosis, pyroptosis, and necrosis: mechanistic description of dead and dying eukaryotic cells," *Infect. Immun.* **73**, 1907–1916 (2005).
74. W. A. High, M. J. Larson, and M. P. Hoang, "Idiopathic bilateral auricular ossificans: a case report and review of literature," *Arch. Pathol. Lab Med.* **128**, 1432–1434 (2004).
75. D. Markovich, "Physiological roles and regulation of mammalian sulphate transporters," *Physiol. Rev.* **81**, 1499–1533 (2001).
76. H. J. Lee, S. V. Balasubramanian, H. Murer, J. Biber, and M. A. Morris, "Modulation of sulfate renal transport by alterations in cell membrane fluidity," *J. Pharm. Sci.* **88**, 976–980 (1999).
77. M. Shinitzky, "Membrane fluidity and cellular functions," in *Physiology of Membrane Fluidity*, M. Shinitzky, Ed., pp. 1–52, CRC Press, Boca Raton, FL, (1984).
78. M. J. G. Bolt, W. Liu, G. Qiao, J. Kong, W. Zheng, T. Krausz, G. Cs-Szabo, M. D. Sitrin, and Y. C. Li, "Critical role of vitamin D in sulphate homeostasis: regulation of the sodium-sulfate cotransporter by 1,25-dihydroxyvitamin D_3," *Am. J. Physiol. Endocrinol. Metab.* **287**, E744–E749 (2004).